Functionalizing Magnet Additive Manufacturing with *In-situ* Magnetic Field Source

Abhishek Sarkar[1], Somashekara M.A.[1], M. Parans Paranthaman[2], Matthew Kramer[1], Christopher Haase[1] and Ikenna C. Nlebedim[1,*]

[1]Critical Materials Institute, Ames Laboratory, United States DOE, Ames, IA, 50011, USA
[2] Oak Ridge National Laboratory, Oak Ridge, TN 37831, USA

Abstract

Additive manufacturing via 3-D printing technologies have become a frontier in materials research, including its application in the development and recycling of permanent magnets. This work addresses the opportunity to integrate magnetic field sources into 3-D printing process in order to enable printing, alignment of anisotropic permanent magnets or magnetizing of magnetic filler materials, without requiring further processing. A non-axisymmetric electromagnet-type field source architecture was designed, modelled, constructed, and installed to a fused filament commercial 3-D printer and tested. The testing was performed by applying magnetic field while printing composite anisotropic Nd-Fe-B+Sm-Fe-N powders bonded in Nylon12 (65vol.%) and recycled Sm-Co powder bonded in PLA (15vol.%). Magnetic characterization indicated that the degree-of-alignment of the magnet powders increased both with alignment field strength (controlled by the current applied to the magnetizing system) and the printing temperature. Both coercivity and remanence were found to be strongly dependent on the degree-of-alignment except for printing performed below but near the Curie temperature of Nd-Fe-B (310°C). Under applied field of 0.15 kOe, Sm-Co and hybrid Nd-Fe-B/Sm-Fe-N printed samples showed degrees-of-alignment of 83% and 65%, respectively. The variations in coercivity were consistent with previous observations in bonded magnet materials. This work verifies that integration of magnetic field sources into 3-D printing processes will result in magnetic alignment of particles while ensuring that other advantages of 3-D printing are retained.

Keywords: 3-D printing; Bonded magnets; In-situ alignment; Magnetic material recycling

1. Introduction:

Additive manufacturing (AM) is a trending technology for rapid-prototyping and fabrication of net-shaped components. It is being significantly studied for application in the manufacturing of permanent magnets and other magnetic materials [1–5]. By avoiding the losses in subtractive manufacturing, AM processes could reduce materials waste and energy consumption. Also, they have the benefits of minimizing or eliminating post-manufacturing machining and tooling typically required for conventional manufacturing [6–8]. In addition to production of permanent magnets, AM has been used as a tool for materials discovery enabled via the laser engineered net-shaping (LENS®) process [9,10]. The LENS® AM system has been used to rapidly synthesize Fe-Co alloys with varying compositions, followed by quick assessment of magnetic properties of the binary system [9,11]. A number of additive manufacturing processes have been developed for 3D printing of permanent magnets, including, Fused Deposition Method (FDM) [3,12,13], UV-cured powder technology [14], laser-guided stereolithography [15] and 3D gel-based printing [16]. However, application of 3-D printing additive manufacturing technologies to magnetic materials is still in the developmental stage.

Bonded magnets are conventionally manufactured either by compression molding with a thermosetting binders, or injection molding with a thermoplastic binder [17]. The economic disadvantage of the dies used in conventional molding can be eliminated by applying 3-D printing AM technologies to bonded magnets production [1,18]. In the works by Li et al [2,3,19], Big Area Additive Manufacturing (BAAM) system was found to produce magnets comparable or better in performance than standard injection molding process, while having the potential to eliminate the use of molds [13]. Ink-based 3-D printing technology for fabrication of composite Nd-Fe-B/strontium ferrite ($SrFe_{12}O_{19}$) bonded magnets was demonstrated by Yang et al. [5]. The

authors printed pseudo-plastic slurries of Nd-Fe-B with 20 wt.% of strontium ferrite and proposed the cost effectiveness of ink-based 3-D printing technology. In the work by Gandha et al. [13], the BAAM process was used for 3-D printing of 65 vol.% of Dy-free anisotropic Nd-Fe-B and Sm-Fe-N composite in Nylon12. They have explored possibilities of post-printing alignment, and varied magnetic field from $\mu_0 H = 0.5 – 5$ T at a temperature of 530 K. The aligned 3-D printed magnets were characterized with an energy product of 11.3 MGOe. Instead of post-production magnetic alignment of permanent magnet materials made via 3-D printing technology, the present work targets *in-situ* alignment (i.e. alignment of magnetic easy axes during 3-D printing). Consequently, the costs associated with post-printing alignment can be eliminated.

Ferromagnetic particles in molten viscous polymer flowing through the nozzle of a 3-D printer can be aligned in the direction of an applied magnetic field. Nlebedim et al. [20] reported detailed experimental analysis on the effect of magnetic field and temperature during the alignment of Nd-Fe-B magnets bonded in EVA polymer. The authors' results predicted higher degree of alignment (based on remanence (M_r)-to-saturation magnetization (M_s) ratio) at lower field strength for magnets aligned at higher temperature (above the melting point of EVA). These results were further validated by Khazdozian et al. [21], suggesting that alignment field, $\mu_0 H <$ 1T, is sufficient to align 65 vol.% of Nd-Fe-B magnet particles (Dy-free anisotropic Magfine-MF18P) bonded in Nylon12 to the applied field direction.

The concept of *in-situ* alignment mechanism for 3-D printed magnets is based on the rotation of magnetic particles in the nozzle of the 3-D printer due to an applied magnetic field. Fig. 1 provides a schematic, illustrating the alignment process as magnet particles move down an

extruder through a region of an applied magnetic field. The polymer matrix which binds the randomly oriented magnet particles in a filament melts as it passes through the nozzle of the extruder. As a result, the mobility of the magnet particles increase and an applied magnetic field can then rotate the particles in its direction as the molten polymer flows through the field source. The challenge is to control the printing conditions (temperature, inlet load and applied magnetic field) in order to maximize the effect of the torque created by the field against the drag torque from the viscosity of the binder. As a result, the magnetic particles can rotate to the field direction as the molten composite flows through the location of the field source at the nozzle.

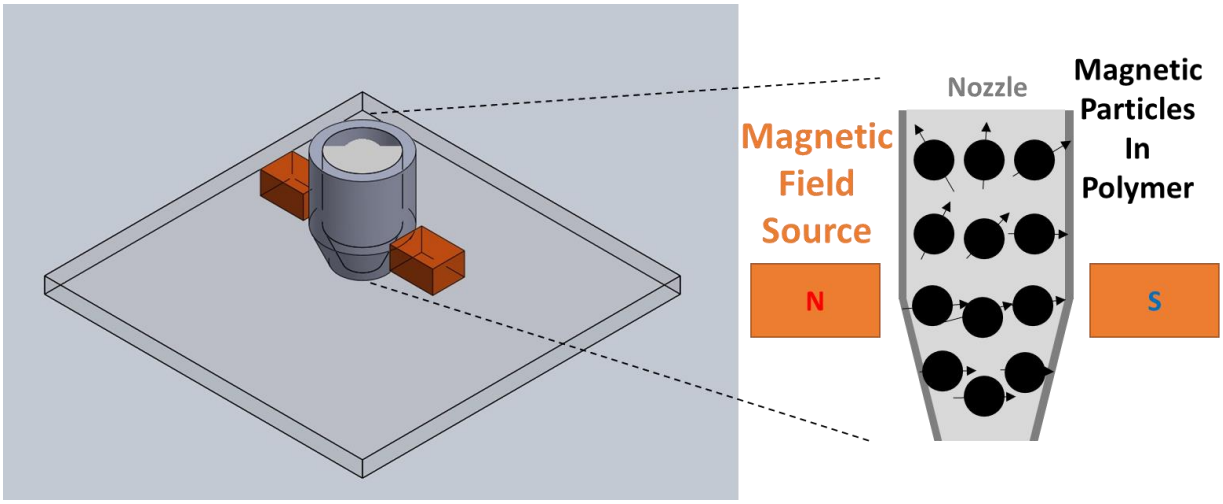

Fig. 1. Schematic of *in-situ* alignment mechanism for 3-D printed magnetic materials.

This work promotes the concept of *in-situ* magnetic alignment of 3-D printed magnetic materials and includes: (a) finite element analysis for the design of an *in-situ* electromagnet alignment system, (b) prototyping and testing of the system, (c) extrusion of magnetic filaments, (d) 3-D printing and magnetic alignment of 65 vol.% composite Nd-Fe-B/Sm-Fe-N in Nylon12 and also recycled 15 vol.% Sm-Co in polylactic acid (PLA), using a commercial-grade fused filament 3-D

printer, (e) magnetic characterization of the 3-D printed parts, and (f) future considerations for 3-D printing in magnetic field.

2. Finite-element Modeling and Prototyping of Electromagnetic Field Source

The first step towards development of the *in-situ* alignment system for additively manufactured bonded magnets was the design, modeling and prototyping of the electromagnetic field source to be installed on a commercial 3-D printer. The electromagnet design used a cold-rolled AISI1010 steel core material and copper wire windings with goal of maximizing magnetic flux concentration and minimizing size, weight and applied electric current. A direct electric current of fixed amperage was employed so coils can safely be used at lower current than rated for the design.

Several electromagnet architectures were developed and studied using Infolytica MagNet v7.9 as represented in Fig. S1 with the magnetic induction contour plots in Fig. S2. The designs were focused on maximizing the field strength along the radial (x) and axial (z) directions, and achieving uniform field distribution near the print-head/platform. Fig. S1(a, b) were designed as a C-core electromagnet and permanent magnet with field varying along the height (axial) direction. The field produced in either of the two models (Fig. S2(a, b)) were not sufficient considering the distance from the bed. A linear Halbach array was designed in Fig. S1(c) to accentuate the flux concentration towards the base. This amplified the field strength of the magnets near the poles (Fig. S2(c)), but the decay of field with distance was larger. Fig. S1(d, e) were designed to be cylindrical Halbach arrays having radial and axial flux concentration, respectively. For the two designs, the magnetic field strength (Fig. S2(d, e)) and its distributions were not desirable because the field directions were axially symmetrical. This meant that the

field direction was radial and symmetric along the cross-section. These models could be applicable as field source for a different 3-D printer. The final two models were the most promising where Fig. S1(f) and Fig. S2(f) was called a two-coil unidirectional magnetizer and Fig. S1(g) and Fig. S2(g) was called a four-coil bidirectional magnetizer. The bidirectional magnetizer model was designed to fit around a nozzle and alternate/rotate about the axis in order to enable multidirectional magnetic field application (like Halbach arrays). Models in Fig. S1(f, g) can be applicable for a larger, industrial-grade 3-D printing system like the BAAM printer, being used in the Manufacturing and Demonstration Facility at Oakridge National Laboratory. However, these designs (Fig. S1(f, g)) were not a geometric fit on the existing MakerGear M2 3D printer without extensive redesigning of the printing unit.

For the purpose of the work herein presented, a non-axisymmetric C-core magnetization architecture was fabricated for a MakerGear M2 or similar 3-D printers. The schematic of the design is presented in Fig. 2(a). The C-core was designed to be non-axisymmetric to maximize the area covered by the nozzle over the printer bed. Considering the magnetic induction formulation for a solenoid in Eq. 1, and optimizing for ease of fabrication, coil weight and thickness, a CAD model for the electromagnet was developed in Solidworks. The estimated mass of the electromagnet unit was 4.5kg.

$$B = \mu H = \mu \frac{NI}{L} \tag{1}$$

Where, B is magnetic induction, μ is the permeability of the core material, μ_0 is the permeability of free space, H is magnetic field, N is the number of turns ($N = \beta^2 Lw$), β is the number of turns per unit length for a wire gauge, I is the applied current, and L, w are the length and width of the coil winding.

The 2D FEA was performed using Infolytica MagNet v7.9. The cold-rolled steel for the non-axisymmetric C-core of the magnetization system was modeled to be wound with 2500turns of AWG22 copper coils and to sustain a maximum amperage of 4A. Fig. 2(b) shows the magnetic field/flux plots obtained by FEA for the electromagnet when only 1A of current was applied to the copper coils. The FEA calculations predicted average magnetic field (H) = 1.8kOe to be produced in the air-gap between the poles of the electromagnet at the 1A current. The FEA parameters are shown in Table 1.

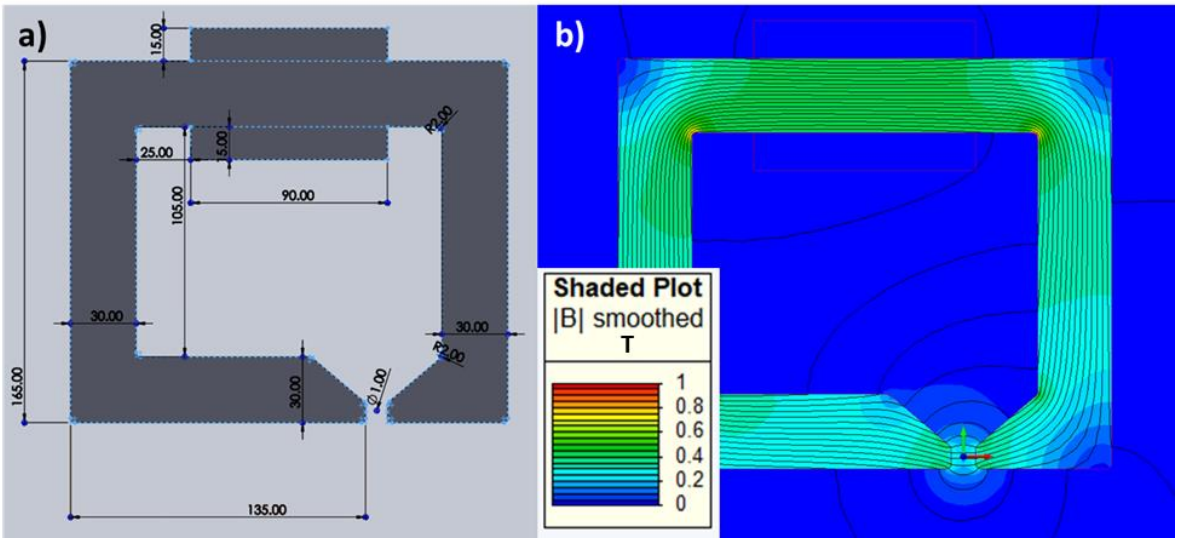

Fig. 2. a) Schematic of C-core electromagnet design for MakerGear M2 3-D printer, and b) Magnetic induction (units in Tesla) and flux contour plots for C-core electromagnet.

The parameters in Table 1 were also used for prototyping the C-core electromagnet. The coils were wound on the AISI1010 steel core material. The electromagnet assembly was mounted on the nozzle head of the 3-D printer using end caps fixtures printed with the printer (Fig. S3). Fig. 3(a) represents the installed electromagnet assembly on the 3-D printer. The movement of the mounted electromagnet towards the ends of 3-D printer's nozzle-bench assembly was restricted to eliminate the possibility of it crashing onto the end supports.

Table 1. Design parameters for the C-core electromagnet.

Parameters	**Values**
Core material	AISI1010 Steel
Winding material	AWG22 Copper
Winding length, $L\ (mm)$	150
Winding thickness, $w\ (mm)$	50
Coils per unit length, $\beta\ (\#/mm)$	1.55
Number of turns, $N\ (\#)$	2500
Assembly weight, (kg)	4.70

The electromagnet core was excited with a Kepco model KLN 150-10 DC power supply. The magnetic field strength generated with the electromagnet was measured for different excitation currents using a FW Bell 5080 gaussmeter (Fig. S4). The applied direct current was varied from 0.50A to 2.00A with steps of 0.25A. The field profiles across the width of the air-gap are plotted in Fig. 3(b). The average field generated for 1A of applied current was found to be 1.54kOe, which was close to the predicted results from FEM (Fig. 2(b)) considering variations in fabricating and uncertainties in the model. For all the applied current in Fig. 3(b), uniform magnetic field was achieved over the 4 mm nozzle diameter, indicating the potential for uniform alignment of magnetic particles during 3-D printing. The magnetic field uniformity over the nozzle increases as the field strength is reduced. For all the applied electric current in Fig. 3(b)., uniform magnetic field was achieved across central 4 mm including nozzle taper (~3 mm) and nozzle hole diameter(~1 mm), indicating the potential for uniform alignment of magnet particles during 3-D printing. The distance between the electromagnet poles over which uniform magnetic field strength was obtained increases with reducing current.

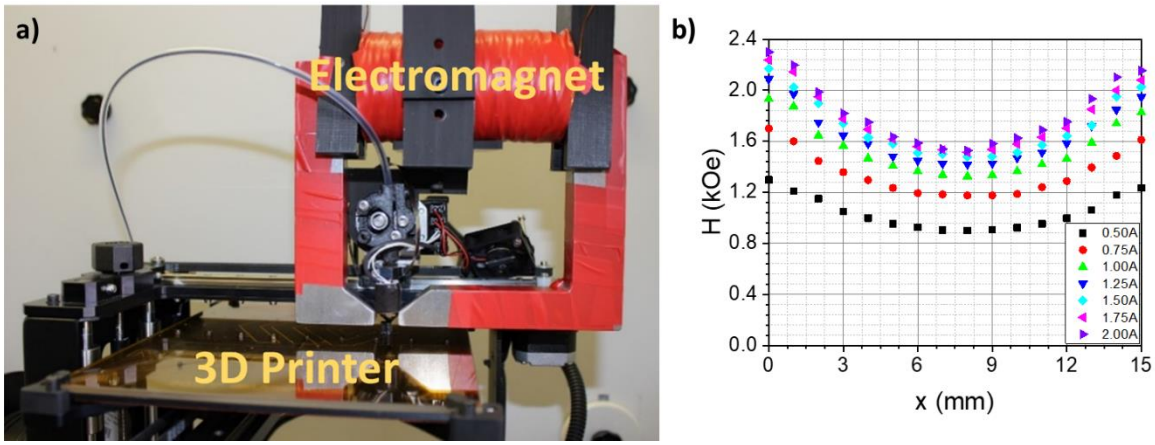

Fig. 3. a) *In-situ* alignment setup prototype with C-core electromagnet on MakerGear M2 printer, and b) Experimental field profile for C-core electromagnet for different alignment currents.

3. Filament preparation and 3-D printing with *in-situ* alignment:

Commercially available filaments are generally made of polylactic acid (PLA) and acrylonitrile butadiene styrene (ABS). However, it is possible to create composite filaments of polymer matrix with desired material as the dispersed phase. In the current analysis, two different filament materials were used. The first material used was pellets of hybrid magnet containing 65vol.% Nd-Fe-B and Sm-Fe-N bonded in Nylon12. The pellets were obtained from NICHIA Corporation. The second material was a composite of recycled samarium cobalt (Sm-Co) in PLA, made using industrially generated Sm-Co swarfs and PLA pellets, as follows. About 46.35g of PLA pellets were dissolved in 100ml of dichloromethane (DCM) while being mechanically homogenized at 150rpm to obtain a viscous solution using Waverly OS20S overhead stirrer. 15vol.% of the recycled Sm-Co grinding swarfs (53.65g) were added to the dissolved PLA/DCM solution. The mixture was stirred while the DCM was evaporated in a fume hood at room temperature (Fig. 4(a)). Afterwards, the dried Sm-Co/PLA was broken down into pellet-sized pieces of arbitrary shape (averaging <5mm in size). The as-received Nd-Fe-B+Sm-Fe-N/Nylon 12 pellets were extruded in Filabot 2.0 extruder (Fig. 4(b)) at $180°C$ to form

1.75mm filaments (Fig. 4(c)). The Sm-Co/PLA pellets were also extruded at 180°C to form 1.75mm filaments (Fig. 4(d)).

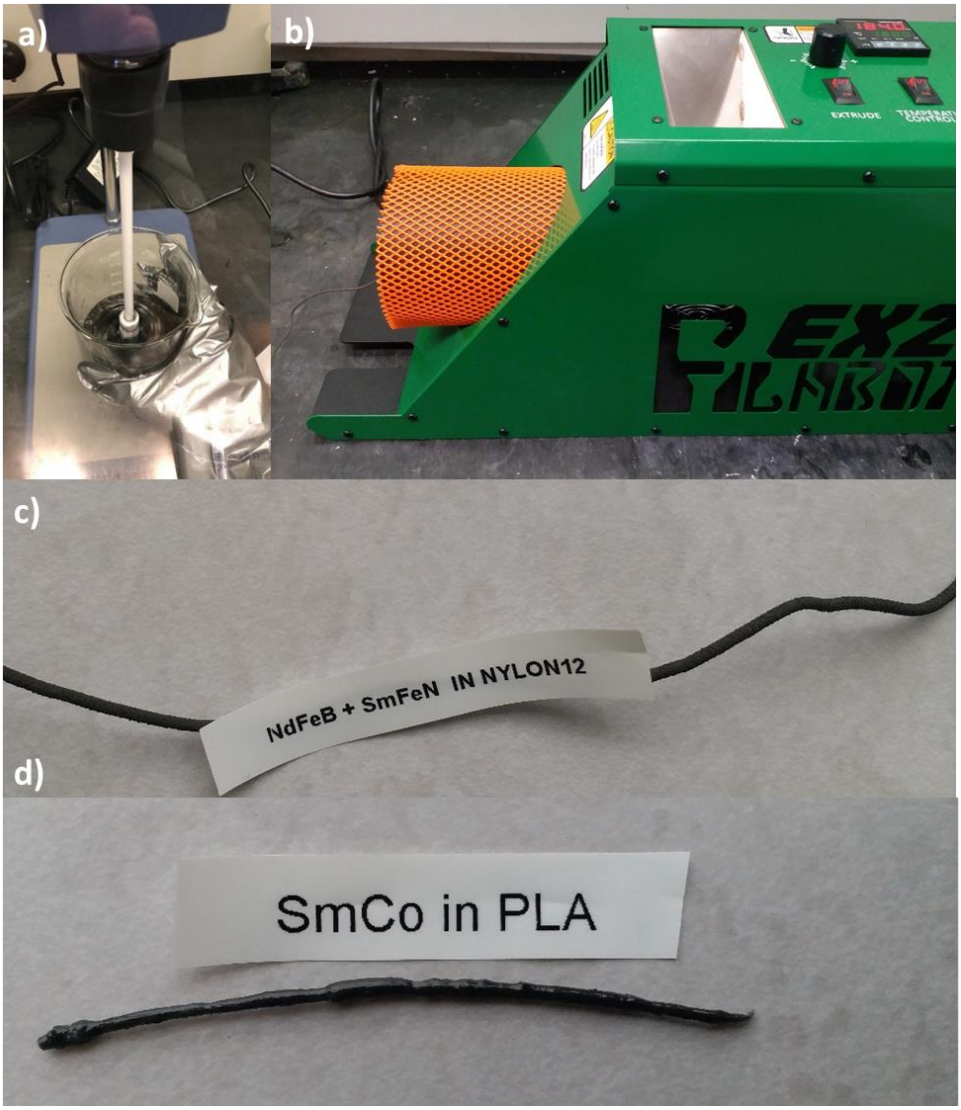

Fig. 4. a) Sm-Co/PLA pellet synthesis process in DCM using mechanical stirrer, b) Extrusion of filament using Filabot 2.0 extruder, c) Nd-Fe-B+Sm-Fe-N/Nylon 12 65vol.% filament, and d) Sm-Co/PLA 15vol.% filament.

The filament was used for the 3-D printing process in the MakerGear M2 3-D printer (Fig. 5(a)) while producing magnetic field with the mounted electromagnet. To determine the onset of softening and melting temperature of the polymer matrix, differential scanning calorimetry (DSC) was performed, with two thermal cycles between $40°C$ and $240°C$. (Fig. 5(b)) shows that

the Nylon12 binder material for the hybrid Nd-Fe-B+Sm-Fe-N/Nylon12 would soften around $160°C$ and start to melt at ~$180°C$. The DSC results were used as a benchmark to determine the lowest printing temperature for the sample.

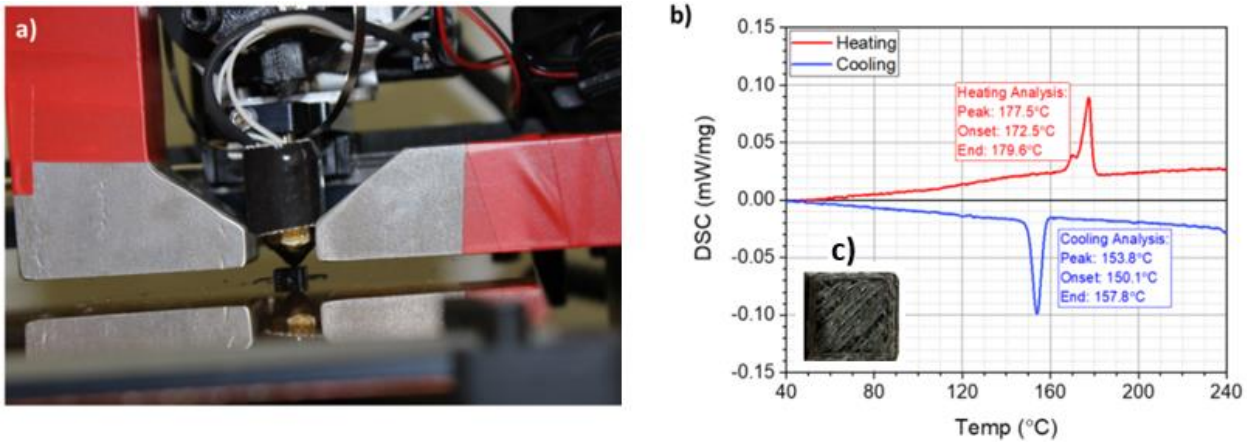

Fig. 5. a) 3-D printing process of filament under magnetic field, b) DSC measurements of Nd-Fe-B+Sm-Fe-N/Nylon12 sample, and c) Printed samples of aligned Sm-Co/PLA at 1.00A.

A CAD model of the bonded magnet to be printed was imported into the Simplify3D software of the 3-D printer, and the nozzle was set to temperature. For each magnet composition, a small square shaped bonded magnet of 10mm x 5mm x 5mm (Fig. 5(c)) was printed. For the Nd-Fe-B/Sm-Fe-N/Nylon12 filaments, printing was performed at different printing temperatures, 180, 230, 275 and 300°C and at a fixed alignment current of 1.50A (corresponding to magnetic field of 1.8kOe). Printing was also performed at a fixed temperature of 180°C and varying alignment currents of 0.0, 0.25, 0.50, 1.00 and 1.50A. The bed temperature, printing speed and inlet load of the filament fixed at 70°C, 100 mm/s and 1.5kg, respectively. Since, the loading fraction for the Nd-Fe-B+Sm-Fe-N/Nylon12 was high (65vol.%), it was difficult to extrude the filament through the 3-D printer nozzle. For the Sm-Co/PLA composite, the nozzle was maintained at 215°C and the bed at 70°C. Due to the lower loading (15 vol.%) of the recycled Sm-Co, compared to the

hybrid Nd-Fe-B+Sm-Fe-N (65 vol.%), an inlet load of 0.5kg was maintained on the filament. Alignment for 3-D printing of the Sm-Co /PLA composite was performed at a fixed field corresponding to applied current of 1A.

4. Magnetic Characterization and Discussion:

The 3-D printed bonded magnet samples of both the hybrid Nd-Fe-B+Sm-Fe-N/Nylon12 and recycled Sm-Co/PLA were characterized using the Vibrating Sample Magnetometer (VSM) mode of Quantum Design Magnetic Property Measurement System (MPMS) system. All samples were measured for their magnetic properties at 27°C with the measurement field varying from -7T to 7T. The error range in all experiments were found to be within 0.1%. The effects of nozzle temperatures on the magnetic properties of the printed nylon bonded Nd-Fe-B+Sm-Fe-N magnets are shown in Fig. 6. Fig. 6(a) shows the magnetic hysteresis plots for samples printed without the application of magnetic field. It shows that printing at temperatures between 180 – 275°C did not degrade the magnetic properties. However, lower coercivity and magnetization were observed at 300°C. Although the 3-D printing was performed in air, it unlikely that the reduced coercivity and magnetization are related to compositional changes in either the Nd-Fe-B or the Sm-Fe-N phases of the magnet powders. Oxidation of Nd-Fe-B and/or Sm-Fe-N or the decomposition of Sm-Fe-N should result in the formation of α-Fe which, in turn, should lead to an increase in magnetization, rather than a decrease. These changes in magnet performance at 300°C may be related to the effect of redistribution of magnet powders. At elevated temperature, the viscosity of the Nylon12 becomes very small which reduces the dispersion of the particles in the binder. Such redistribution promotes particle-to-particle interactions which has been shown to affect magnetic performance of bonded magnets as explained by Nlebedim et al [20].

When viscoelastic drag is lowered at elevated temperatures and magnetic field is simultaneously applied, alignment of magnetic easy axes to the applied field direction should result in increase in magnetization. This is readily seen by comparing magnetization values at similar field strengths (e.g. 70kOe) in Fig. 6(b) with Fig. 6(a). Fig. 6(c) shows that the degree of alignment increased with printing temperature. The degree of alignment was defined as the value of the ratio of remanence (M_r) to magnetization at the maximum applied magnetic field of 70kOe ($M@7T$). Near the Curie temperature (Tc) of Nd-Fe-B (~310°C), the randomizing effect of thermal energy should surpass the alignment effects of the applied magnetic field. Hence, printing at 300°C would result in less efficient alignment of the magnetic easy axes of the powders to the field direction, compared with printing at temperatures well below the Curie temperature. Nevertheless, the printing temperature should also be sufficiently high to reduce the viscosity of the binder and allow the particles to rotate. Consistent with decreased magnetization at 300°C, M_r also decreased at the same printing temperature, as also shown in Fig. 6(c). The maximum degree of alignment achieved for Nd-Fe-B+Sm-Fe-N in Nylon12 sample is 65% at print temperature of 300°C. The intrinsic coercivity trend in Fig. 6(d) is similar to previous reports [20] and suggests that printing temperatures below 220°C, coercivity mechanism is dominated by the nucleation demagnetization process (i.e. Stoner-Wolfhart mechanism): coercivity increases with alignment field. Above printing temperatures of 220°C, domain wall displacement demagnetization process (i.e. Kondorski mechanism) dominated: coercivity decreases with increasing degree of alignment.

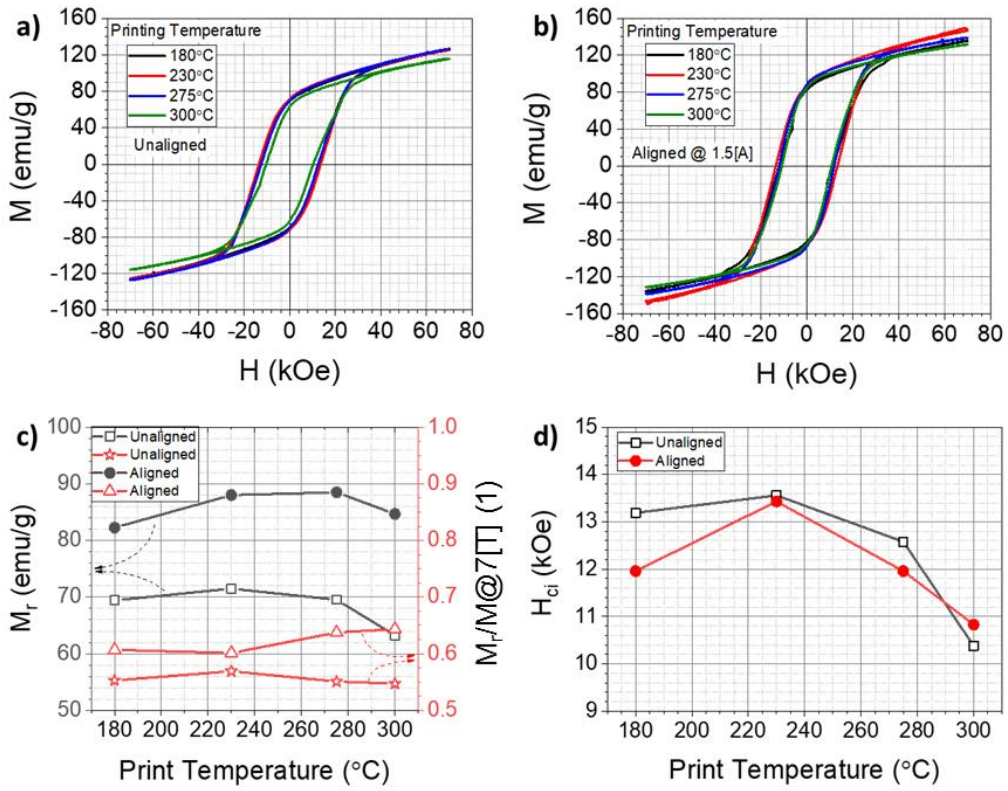

Fig. 6. MH loop for 3-D printed Nd-Fe-B+Sm-Fe-N/Nylon12 65vol.%, a) Varying nozzle temperature at 0A alignment current, b) Varying nozzle temperature at 1.50A alignment current, c) Varying alignment current for 180°C nozzle temperature, and d) Perpendicular and parallel magnetization at 230°C and 1.50A alignment current.

Fig. 7 shows the effect of varying applied magnetic field (by varying applied electric current) on the degree of alignment, remanence and coercivity, at printing temperature of $180°C$. The hysteresis loops in Fig. 7(a). shows that magnetization consistently increased with applied magnetic field, during 3-D printing due to increasing decree of alignment (Fig. 7(b)). The increase in degree of alignment should also result in increased M_r, as shown in Fig. 7(b). It is unclear why the coercivity initially decreased between the sample printed without magnetic field and the sample printed at magnetic field strength corresponding to applied current of 0.25A. However, Fig. 7(b) suggests that the competition between the two demagnetization processes described above is both temperature and field dependent.

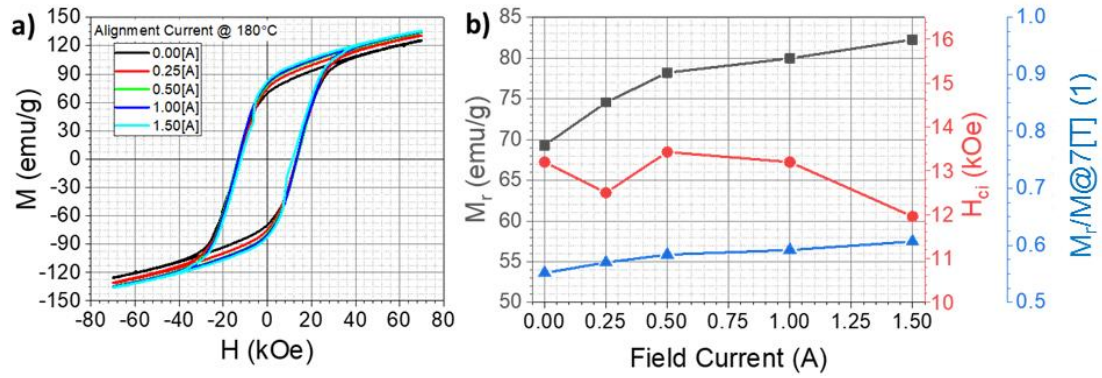

Fig. 7. a) Magnetic characterization of Nd-Fe-B+Sm-Fe-N/Nylon12 65vol.% sample printed at 180ºC nozzle temperature under varying alignment current, and b) Remanence, coercivity and Mr/Ms variation for Nd-Fe-B+Sm-Fe-N/Nylon12 65vol.% sample with field current.

Fig. 8 shows magnetization vs. magnetic field measured both parallel and perpendicular to the direction of magnetic alignment for a select sample printed at 230°C and at magnetic field strength corresponding to 1.5A of applied current. The reduced magnetization in the perpendicular direction, compared to the parallel direction, further confirms the orientation of the magnetic easy axes to the applied field direction during 3-D printing.

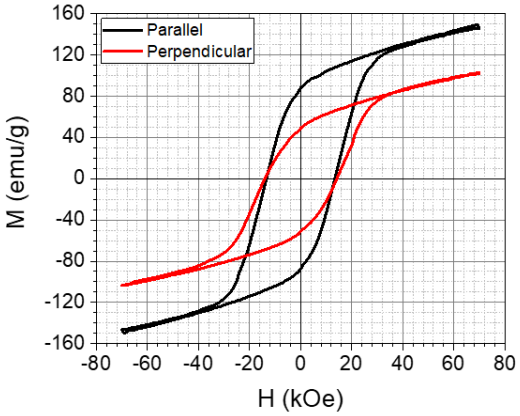

Fig. 8. Magnetic characterization of Nd-Fe-B+Sm-Fe-N/Nylon12 65vol.% sample aligned at 230ºC nozzle temperature and 1.5A alignment current.

The potential for extending 3-D printing in magnetic field to the recycling of industrially generated magnet swarfs was demonstrated using 15 vol.% of Sm-Co bonded in PLA. Swarfs are magnet fillings generated during post-production operations such as grinding, polishing, etc. Fig. 9 shows the magnetization vs. applied field plot for a sample printed as described in the experimental section. As expected, Fig. 9(a) shows isotropic magnetization vs. magnetic field for sample printed without magnetic field. Printing in magnetic field resulted in magnetic anisotropy in the magnet, hence the differences in magnetization for measurements in the parallel and perpendicular directions. The coercivity values are 12.2kOe for the isotropic sample, 9.3kOe and 13.2kOe for the anisotropic sample measured in the parallel and perpendicular directions, respectively. The degree of alignment achieved for the Sm-Co in PLA sample was 83%.

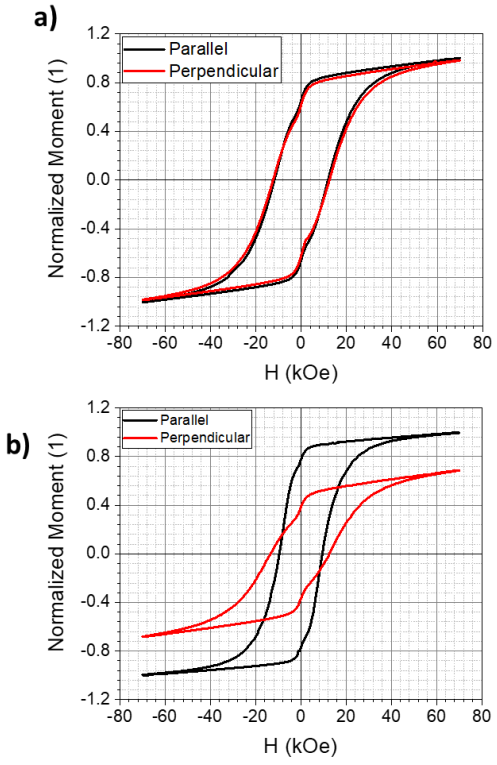

Fig. 9. Normalized MH loop for Sm-Co/PLA 15vol.% 3-D printed sample, a) unaligned, and b) aligned at 1.00A alignment current.

5. Future Applications:

The primary application of the concept of *in-situ* alignment of 3-D printed magnets is to prototype net-shaped magnets with complex alignment requirements. The concept could also be applicable for net-shaping of soft magnet-based and bio-inspired composites [22,23]. Soft magnetic materials in polymer matrix could be shaped using the alignment field of the electromagnet and upon solidification, the material would be conformed in the desired shape. Magnetic templating would be another area in which *in-situ* alignment technique could be applicable for 3-D printing. The work done by Sander et al. for magnetic templating lithium electrodes, could be combined with 3-D printing of electrode to allow *in-situ* pore alignment while 3-D printing of electrodes [24,25]. Therefore, the mechanism could be applied for *in-situ* channeling of 3-D printed structures.

6. Conclusions:

The novel concept of *in-situ* magnetic alignment for 3-D printed magnets was demonstrated with a non-axisymmetric C-core electromagnet, modeled using FEM, prototyped and integrated into a commercial 3-D printer. 65 vol.% of Nd-Fe-B+Sm-Fe-N in Nylon12 was printed in magnetic field and at different nozzle temperatures and applied field strengths. 15 vol.% of Sm-Co in PLA was also printed in magnetic field in order to demonstrate the extensibility of the system to recycling of waste permanent magnet materials. For both material types, the effect of applied field in orienting the particles of the anisotropic magnet powders to the magnetic field direction was demonstrated. The degree of alignment of the magnet powders to the field direction was found to be a function of both the applied magnetic field and printing temperature. The work demonstrates

the concept of *in-situ* alignment of magnetic materials in fused-filament 3-D printers for prototyping of permanent magnets.

Acknowledgement:

This work is supported by the Critical Materials Institute (CMI), an Energy Innovation Hub funded by the U.S. Department of Energy (DOE), Office of Energy Efficiency and Renewable Energy, Advanced Manufacturing Office. Ames Laboratory is operated for the U.S. Department of Energy by Iowa State University of Science and Technology under Contract No. DE-AC02-07CH11358. Authors are thankful to Electron Energy Corporation for providing the Sm-Co grinding swarfs used for this work. Authors also appreciate Dr. Thomas Lograsso for his guidance during the conceptualization of this work.

References:

[1] C. Huber, C. Abert, F. Bruckner, M. Groenefeld, O. Muthsam, S. Schuschnigg, C. Vogler, R. Windl, D. Suess, 3D print of polymer bonded rare-earth magnets , and 3D magnetic field scanning with an end-user 3D printer, Appl. Phys. Lett. 109 (2016) 162401. https://doi.org/10.1063/1.4964856.

[2] L. Li, A. Tirado, B.S. Conner, M. Chi, A.M. Elliott, O. Rios, H. Zhou, M.P. Paranthaman, A novel method combining additive manufacturing and alloy infiltration for NdFeB bonded magnet fabrication, J. Magn. Magn. Mater. 438 (2017) 163–167. https://doi.org/10.1016/j.jmmm.2017.04.066.

[3] L. Li, A. Tirado, I.C. Nlebedim, O. Rios, B. Post, V. Kunc, R.R. Lowden, E. Lara-Curzio, R. Fredette, J. Ormerod, T.A. Lograsso, M.P. Paranthaman, Big Area Additive

Manufacturing of High Performance Bonded NdFeB Magnets, Sci. Rep. 6 (2016) 36212. https://doi.org/10.1038/srep36212.

[4] E.A. Périgo, J. Jacimovic, F. García Ferré, L.M. Scherf, Additive manufacturing of magnetic materials, Addit. Manuf. 30 (2019) 100870. https://doi.org/10.1016/j.addma.2019.100870.

[5] F. Yang, X. Zhang, Z. Guo, S. Ye, Y. Sui, A.A. Volinsky, 3D printing of NdFeB bonded magnets with SrFe 12 O 19 addition, J. Alloys Compd. 779 (2019) 900–907. https://doi.org/10.1016/j.jallcom.2018.11.335.

[6] R. Leal, F.M. Barreiros, L. Alves, F. Romeiro, J.C. Vasco, M. Santos, C. Marto, Additive manufacturing tooling for the automotive industry, Int. J. Adv. Manuf. Technol. 92 (2017) 1671–1676. https://doi.org/10.1007/s00170-017-0239-8.

[7] B. Nagarajan, A.F. Eufracio Aguilera, M. Wiechmann, A.J. Qureshi, P. Mertiny, Characterization of magnetic particle alignment in photosensitive polymer resin: A preliminary study for additive manufacturing processes, Addit. Manuf. 22 (2018) 528–536. https://doi.org/10.1016/j.addma.2018.05.046.

[8] C. Klahn, B. Leutenecker, M. Meboldt, Design Strategies for the Process of Additive Manufacturing, Procedia CIRP. 36 (2015) 230–235. https://doi.org/10.1016/j.procir.2015.01.082.

[9] C. V. Mikler, V. Chaudhary, T. Borkar, V. Soni, D. Jaeger, X. Chen, R. Contieri, R. V. Ramanujan, R. Banerjee, Laser Additive Manufacturing of Magnetic Materials, JOM. 69 (2017) 532–543. https://doi.org/10.1007/s11837-017-2257-2.

[10] T. Borkar, R. Conteri, X. Chen, R. V. Ramanujan, R. Banerjee, Laser additive processing of functionally-graded Fe–Si–B–Cu–Nb soft magnetic materials, Mater. Manuf. Process. 32 (2017) 1581–1587. https://doi.org/10.1080/10426914.2016.1244849.

[11] J. Geng, I.C. Nlebedim, M.F. Besser, E. Simsek, R.T. Ott, Bulk Combinatorial Synthesis and High Throughput Characterization for Rapid Assessment of Magnetic Materials: Application of Laser Engineered Net Shaping (LENS^{TM}), JOM. (2016). https://doi.org/10.1007/s11837-016-1918-x.

[12] M.P. Paranthaman, C.S. Shafer, A.M. Elliott, D.H. Siddel, M.A. McGuire, R.M. Springfield, J. Martin, R. Fredette, J. Ormerod, Binder Jetting: A Novel NdFeB Bonded Magnet Fabrication Process, JOM. 68 (2016) 1978–1982. https://doi.org/10.1007/s11837-016-1883-4.

[13] K. Gandha, L. Li, I.C. Nlebedim, B.K. Post, V. Kunc, B.C. Sales, J. Bell, M.P. Paranthaman, Additive manufacturing of anisotropic hybrid NdFeB-SmFeN nylon composite bonded magnets, J. Magn. Magn. Mater. (2018). https://doi.org/10.1016/j.jmmm.2018.07.021.

[14] A. Shen, C.P. Bailey, A.W.K. Ma, S. Dardona, UV-assisted direct write of polymer-bonded magnets, J. Magn. Magn. Mater. 462 (2018) 220–225. https://doi.org/10.1016/j.jmmm.2018.03.073.

[15] E.M.H. White, A.G. Kassen, E. Simsek, W. Tang, R.T. Ott, I.E. Anderson, Net Shape Processing of Alnico Magnets by Additive Manufacturing, IEEE Trans. Magn. 53 (2017) 1–6. https://doi.org/10.1109/TMAG.2017.2711965.

[16] F. Yang, X. Zhang, Z. Guo, A.A. Volinsky, 3D gel-printing of Sr ferrite parts, Ceram. Int. 44 (2018) 22370–22377. https://doi.org/10.1016/j.ceramint.2018.08.364.

[17] J. Ormerod, S. Constantinides, Bonded permanent magnets: Current status and future opportunities (invited), J. Appl. Phys. 81 (1997) 4816. https://doi.org/10.1063/1.365471.

[18] L. Li, B. Post, V. Kunc, A.M. Elliott, M.P. Paranthaman, Additive manufacturing of near-net-shape bonded magnets : Prospects and challenges, Scr. Mater. 135 (2017) 100–104. https://doi.org/10.1016/j.scriptamat.2016.12.035.

[19] L. Li, K. Jones, B. Sales, J.L. Pries, I.C. Nlebedim, K. Jin, H. Bei, B.K. Post, M.S. Kesler, O. Rios, V. Kunc, R. Fredette, J. Ormerod, A. Williams, T.A. Lograsso, M.P. Paranthaman, Fabrication of highly dense isotropic Nd-Fe-B nylon bonded magnets via extrusion-based additive manufacturing, Addit. Manuf. 21 (2018). https://doi.org/10.1016/j.addma.2018.04.001.

[20] I.C. Nlebedim, H. Ucar, C.B. Hatter, R.W. McCallum, S.K. McCall, M.J. Kramer, M.P. Paranthaman, Studies on in situ magnetic alignment of bonded anisotropic Nd-Fe-B alloy powders, J. Magn. Magn. Mater. 422 (2017) 168–173. https://doi.org/10.1016/j.jmmm.2016.08.090.

[21] H.A. Khazdozian, L. Li, M.P. Paranthaman, S.K. McCall, M.J. Kramer, I.C. Nlebedim, Low-Field Alignment of Anisotropic Bonded Magnets for Additive Manufacturing of Permanent Magnet Motors, JOM. (2019). https://doi.org/10.1007/s11837-018-3242-0.

[22] J.J. Martin, B.E. Fiore, R.M. Erb, Designing bioinspired composite reinforcement architectures via 3D magnetic printing, Nat. Commun. (2015).

https://doi.org/10.1038/ncomms9641.

[23] Y. Kim, H. Yuk, R. Zhao, S.A. Chester, X. Zhao, Printing ferromagnetic domains for untethered fast-transforming soft materials, Nature. 558 (2018) 274–279. https://doi.org/10.1038/s41586-018-0185-0.

[24] J.S. Sander, R.M. Erb, L. Li, A. Gurijala, Y.M. Chiang, High-performance battery electrodes via magnetic templating, Nat. Energy. (2016). https://doi.org/10.1038/nenergy.2016.99.

[25] C. Reyes, R. Somogyi, S. Niu, M.A. Cruz, F. Yang, M.J. Catenacci, C.P. Rhodes, B.J. Wiley, Three-Dimensional Printing of a Complete Lithium Ion Battery with Fused Filament Fabrication, ACS Appl. Energy Mater. (2018). https://doi.org/10.1021/acsaem.8b00885.